

Heterogeneous Federated Learning with Group-Aware Prompt Tuning

Wenlong Deng, Christos Thrampoulidis, Xiaoxiao Li
Department of Electrical and Computer Engineering,
The University of British Columbia, Vancouver, BC, Canada
{dwenlong, cthrampo, xiaoxiao.li}@ece.ubc.ca

Abstract

Transformers have achieved remarkable success in various machine-learning tasks, prompting their widespread adoption. In this paper, we explore their application in the context of federated learning (FL), with a particular focus on heterogeneous scenarios where individual clients possess diverse local datasets. To meet the computational and communication demands of FL, we leverage pre-trained Transformers and use an efficient prompt-tuning strategy. Our strategy introduces the concept of learning both shared and group prompts, enabling the acquisition of universal knowledge and group-specific knowledge simultaneously. Additionally, a prompt selection module assigns personalized group prompts to each input, aligning the global model with the data distribution of each client. This approach allows us to train a single global model that can automatically adapt to various local client data distributions without requiring local fine-tuning. In this way, our proposed method effectively bridges the gap between global and personalized local models in Federated Learning and surpasses alternative approaches that lack the capability to adapt to previously unseen clients. The effectiveness of our approach is rigorously validated through extensive experimentation and ablation studies.

1 Introduction

Federated Learning (FL) [23] is a framework that learns machine learning (ML) models from multiple disjoint clients without the need to share their own data. As such, it provides an opportunity for collaborative ML across multiple institutions without risking the leakage of private data. However, FL algorithms suffer from slow model training or divergence when clients' local data distributions are heterogeneous; thus harming the model's performance. In response to this, a significant amount of work has been devoted to understanding and addressing heterogeneity.

One line of heterogeneous FL methods focuses on learning a single global model. To be specific, some variants of FedAvg methods [13, 20, 18] learn a single model by tackling the issues of stability, the shift in the feature space, and client drift. However, relying solely on a single global model may not be sufficient under significant data heterogeneity [18].

Another line of heterogeneous FL research focuses on personalized FL (PFL) that obtains different models personalized to individual users. For example, one approach applies fine-tuning on local client data to adjust a global or meta-trained model to personalized models; another considers client similarity and incorporates clustering clients with similar data distributions, assuming they share the same optimal model [8, 21, 3]. However, these PFL methods face several issues: (1) Fine-tuning-based PFL may lead to overfitting on local data [36]. (2) Cluster-based PFL imposes a heavy computational burden [22, 28]. (3) None of the aforementioned methods can be directly adapted to unseen clients without

further adaptation using locally labeled data, limiting flexibility and efficiency.

To summarize: On one hand, training a single FL model can achieve high generalizability on global and unseen data distributions (*e.g.* by using the first line of methods), but suffers in obtaining satisfying local accuracy in severe heterogeneity. On the other hand, PFL can obtain high local testing performance (*e.g.* by using the second line of methods) but lacks generalizability. To overcome these limitations, our goal is to integrate the advantages of these two types of FL strategies and explore the following critical question: *Can we train a single FL model that not only achieves high accuracy on the global distribution but is also capable of aligning with different local distributions?*

Recently, Transformers [32] have shown to embrace surprising robustness to distribution shifts [2] and computer vision tasks [14]. However, training Transformers in FL presents a unique set of challenges. Firstly, robust training of these models from scratch typically requires a large amount of training data [6]. Secondly, Transformers are inherently parameter-rich, significantly surpassing Convolutional Neural Networks (CNNs) as evidenced in [6]. Thirdly, Transformers' robustness to distribution shift may not be sufficient for good performance when facing strong heterogeneous data distributions and limited training samples in FL. These facts make it challenging to train Transformers in an FL environment, where local data is limited, clients are heterogeneous, and the efficient transmission of large models between servers and clients is a critical concern. Consequently, to successfully incorporate Transformer models in FL, it is imperative to devise suitable strategies that update only a relatively small, appropriate, subset of the parameters, while handling heterogeneous local data distributions.

To address the aforementioned question, we introduce Federated Group-Aware Prompt Tuning (dubbed FGPT), inspired by recent prompt tuning methods [11, 35]. As shown in Fig. 1 (a), FGPT globally learns shared and group prompts, which facilitate the learning of both universal and group-specific knowledge. In the prompt selection module (see Fig.1 (b)), each input is assigned a personalized set of group prompts based on variations in the clients' frequency of group prompt selection (illustrated in Fig.1 (c)). This enables automatically aligning the global model with each local client's data distribution. *Importantly, FGPT can be directly applied to new clients as its personalization could be achieved during the testing time on every testing sample, requiring only one additional inference for prompt selection.*

The contributions of this research can be summarized as follows:

- We introduce FGPT algorithm, which learns a single global model that can achieve good test accuracy on both global data distribution and local clients' data distribution.
- FGPT can be directly applied to new clients without fine-tuning during inference.

- We conducted extensive experiments using different datasets and various extreme non-IID settings. Our results clearly show that FGPT performs better than all the baselines.
- We have developed a theoretical analysis that generalizes the error bound between global and local performance considering the group-structure of data. This analysis has been validated through multiple experiments.

2 Preliminary

2.1 Federated Averaging (FedAvg)

Assume that there is a server that can both send and receive messages from M client devices. Each client i is equipped with its own data distribution \mathcal{D}_i on $\mathcal{X} \times \mathcal{Y}$, where \mathcal{X} is the input space and \mathcal{Y} is the label space with K classes in total. Data (x_j^i, y_j^i) located on participating client i consist of N_i i.i.d samples from \mathcal{D}_i . The objective of classical FL is to minimize the global loss:

$$\arg \min_w \sum_{i=1}^M \frac{1}{M} \sum_{j=1}^{N_i} \frac{1}{N_i} l(w; x_j^i, y_j^i).$$

In FedAvg [23], one of the most popular FL strategies, each client device i undergoes several local updates on its dataset at t -th communication round to obtain updated weights w_i^{t+1} . Then, all clients' models $w_i^{t+1}, i \in [M]^1$ are broadcast to the server. Last, the server aggregates the local models to produce new global model w^{t+1} as follows:

$$w^{t+1} \leftarrow \frac{1}{M} \sum_{i \in [M]} \frac{N_i}{N} w_i^{t+1},$$

where N is the total number of data samples across all clients. This aggregated global model is shared with all clients and the above process is repeated till convergence.

2.2 Visual Prompt Tuning (VPT)

Prompt Tuning is an efficient alternative to fine-tuning full or part of the parameters of large-scale Transformer models. Drawing from recent advances in efficiently tuning large language models, VPT [11] introduces only a small amount (less than 1% of model parameters) of trainable parameters in the input space while keeping the backbone model frozen. VPT-shallow is the most efficient version proposed by VPT, where prompts are inserted into the first Transformer layer L_1 only. Each prompt token is a learnable d -dimensional vector. A collection of p prompts is denoted as $P = \{w_k \in \mathbb{R}^d | k \in \mathbb{N}, 1 \leq k \leq p\}$. Specifically, the VPT-shallow is described as follows:

$$\begin{aligned} [\text{cls}_1, \mathbf{Z}_1, \mathbf{E}_1] &= L_1([\text{cls}_0, \mathbf{P}, \mathbf{E}_0]) \\ [\text{cls}_u, \mathbf{Z}_u, \mathbf{E}_u] &= L_u([\text{cls}_{u-1}, \mathbf{Z}_{u-1}, \mathbf{E}_{u-1}]) \quad i = 2, \dots, U \\ \mathbf{y} &= \text{Head}(\text{cls}_U), \end{aligned}$$

where U is the number of layers, $\mathbf{Z}_u \in \mathbb{R}^{p \times d}$ represents the prompt features computed by the u -th Transformer layer L_u , \mathbf{E}_u is collection of image patch embeddings as inputs to the $(u+1)$ -th Transformer layer L_{u+1} , $\text{cls}_u \in \mathbb{R}^d$ denotes the classification embedding at L_{u+1} 's input space. **Red** and **blue** indicate **learnable** and **frozen** parameters, respectively.

¹For integer m , we denote $[m] = \{0, 1, \dots, m\}$.

3 Method

3.1 Problem Setup

We examine a scenario comprising M clients and a central server. The local clients collaboratively adapt a pre-trained Transformer model using decentralized local client data while safeguarding the privacy of their raw data. To achieve this, we introduce a FL framework with a group-aware prompt-tuning setup. Let us define a function $Select : \mathcal{X} \rightarrow [G]$ that efficiently groups data into G groups. For the model, consider the group prompt set $P_G = \{p_1, \dots, p_G\}$ containing G group prompt $p_g \in \mathbb{R}^d$, where d is the feature dimension and $g \in [G]$. Further let a set P_S of shared prompts containing S learnable prompts with same dimension as p_g . Let classifier weights W_C , and data point (x, y) sampled from \mathcal{D}_i for client $i \in [M]$. Then, the objective is to minimize:

$$\arg \min_{W=\{P_G, P_S, W_C\}} \sum_{i=1}^M \frac{N_i}{N} \mathbb{E}_{(x,y) \sim \mathcal{D}_i} [l(p_g, P_S, W_C; x, y)], \quad (1)$$

where $l : \mathcal{X} \times \mathcal{Y} \rightarrow \mathbb{R}^+$ is the cross-entropy loss, $p_g \in P_G$ are the selected group prompts that aligned with the predicted group membership of input x from the function $Select$. Finally, $W = (P_G, P_S, W_C)$ denotes the collection of all trainable weights with other model parameters frozen.

3.2 Architecture

In this work, we utilize a pre-trained Transformer and adapt it to new tasks by prompt-tuning [11]. We further advanced the model architecture so that it can align to different data distributions automatically.

To be specific, our approach involves learning shared prompts for common features while also employing specialized group prompts through a prompt selection module (explained in detail in Eq.5) to effectively align with various local client data distributions. In Fig.1 (a), we initialize with a pre-trained ViT model comprising U layers and let the L_u represents the u -th layer, \mathbf{E}_u represents the embedding feature of the u -th block, \mathbf{Z}_u^S represents the shared prompt features, and $\text{cls}_u \in \mathbb{R}^d$ denotes the classification embedding at L_{u+1} 's input space. Subsequently, the shared prompts P_S are attached to the embedding features of the 1-st layer to extract universal features:

$$[\text{cls}_1, \mathbf{Z}_1^S, \mathbf{E}_1] = L_1([\text{cls}_0, P_S, \mathbf{E}_0]). \quad (2)$$

Next, we use the $Select$ function to assign group membership $g = Select(x)$ to a sample x (detailed in Eq. 5) and insert corresponding group prompts $p_g \in P_G$ to a higher layer u ($u = 6$ in our case) to extract task-specific features [26]:

$$[\text{cls}_u, z_u^g, \mathbf{Z}_u^S, \mathbf{E}_u] = L_u([\text{cls}_{u-1}, p_g, \mathbf{Z}_{u-1}^S, \mathbf{E}_{u-1}]), \quad (3)$$

where z_u^g represents the group prompt feature computed by the u -th Transformer layer L_u . Similar to the previous visual prompt tuning method [11], we use the cls token from last layer U for classification:

$$\mathbf{y} = \text{Head}(\text{cls}_U). \quad (4)$$

To demonstrate the necessity and diversity of group prompts, we evaluate the prompt similarity among different clients in Table 11, which supports the group prompts help to alleviate gradient dissimilarity.

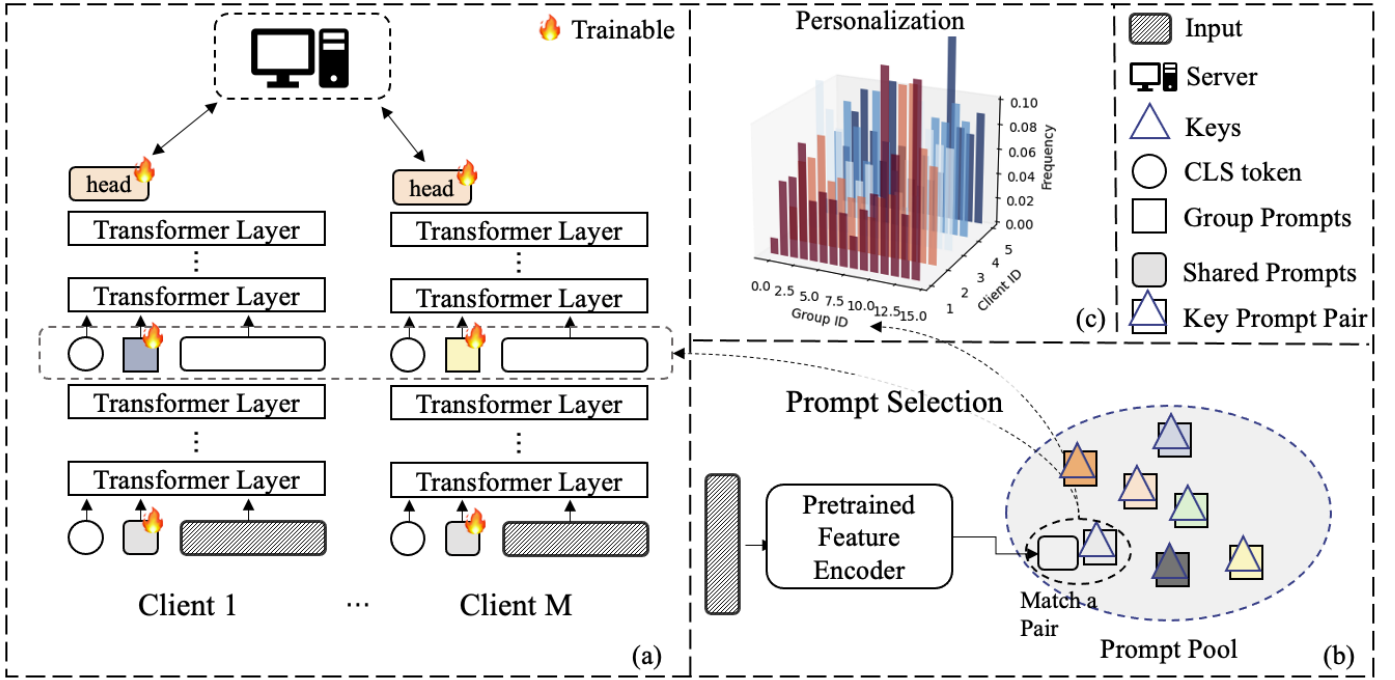


Figure 1: Pipeline of our methods. (a) Provides an overview of the federated group-aware prompt-tuning $FGPT$ procedure. Each model comprises shared prompts and group prompts, facilitating the acquisition of both universal and group-specific knowledge. The shared prompts and classification head are globally trained, while the group prompt is inserted into intermediate layers and trained within its respective data group. (b) Depicts the prompt selection module. Here, each input undergoes processing by a shared-prompt tuned foundation model encoder (e.g., ViT in our case). Similarities between keys and last layer CLS token features are calculated, and the prompt corresponding to the most similar key is selected for training, enabling personalized training at the sample level. (c) Given that data distributions vary across clients, the frequencies of selected group prompts differ, resulting in client-level personalization. This aspect ensures our model aligns on various local data distributions.

3.3 Aligning Prompts with Local Data Distribution

In this section, we introduce the prompt selection module *Select*. The module is inspired by recent prompt tuning methods for continual learning [35, 5, 34], which employ learning of a key for each group $g \in \mathcal{G}$. These keys are trained to capture the similarity to the feature representations within their respective groups. However, in our FL setting, data are divided among multiple clients, making it hard to learn a stable selection module. Here, we propose a simple yet effective approach to tackle these challenges by utilizing a set of predefined orthogonal keys. As shown in Fig. 1 (b), we generate G fixed orthogonal keys $\mathcal{B} = \{b_1, \dots, b_G\}$ which shared globally, and $b_g \in \mathbb{R}^d$ has the same size as the cls token. Then, the function *Select* divides the data into G distinct groups based on the *fixed orthogonal keys* \mathcal{B} using the following formula:

$$Select(x) = \arg \max_g \cos(h_\theta(x), b_g). \quad (5)$$

Here, $h_\theta(x)$ represents the cls token output from the pre-trained foundation model, which generates meaningful semantic features. On one hand, the model can select group prompts according to input sample x , thus embracing the ability to align with various data distributions. On the other hand, data from the same group will update the same group prompt reducing the distribution mismatching as explained in Theorem 5.1.

3.4 Algorithm

In this section, we provide the detailed algorithms of $FGPT$ during the training and testing phase. Furthermore, we introduce a variation of $FGPT$ during inference, named $FGPT-U$ (performance

reported in Table 1), where a test-time ensemble is performed on top of $FGPT$.

Training:

First, we provide a detailed illustration of the training process for our proposed method in Algorithm 1 based on the commonly used FedAvg [23] scheme: during each communication round, the clients engage in local training using the global model received from the server, and the server aggregates the shared parameters from clients to update the global model. Particularly, in $FGPT$'s training, the local model parameters (*i.e.*, P_S and P_G) are sent back to the server for aggregation. For shared parameters, the aggregation weight of client i is determined by $\alpha_i = N_i/N$. Regarding the aggregation of group prompts, we initially calculate the selection frequency of a group g on client i denoted as N_g^i . Then, the aggregation weight β_g^i for the group prompt is computed as $N_g^i / \sum_i N_g^i$. This weight considers the distribution of group prompts across the participating clients.

Inference:

We illustrate the inference procedure of $FGPT$ in Algorithm 2, where one prompt ($K = 1$) is selected for prediction. To be specific, the shared prompts and cls token along with image embeddings are sent into the first layer, and the selected group prompt for the given testing sample is inserted at u -th layer. In order to further reduce the generalization error when splitting data into groups (detailed in Theorem 5.1), we propose $FGPT-U$ for ensemble prediction. The implementation of $FGPT-U$ differs from $FGPT$ only during the inference stage. At this stage, $FGPT-U$ selects the top- K (in our case, Top-5) most

Table 1: Performance comparison of different methods on the CIFAR-100 and CIFAR-100-C Datasets with Pathological partition. We report the averaged testing accuracy for the last 10 consecutive global communication rounds and compute the mean test accuracy and variance over these evaluation steps to estimate the model’s performance. The **bold** and underline highlights represent the best and second best results respectively.

FL settings		Accuracy ↑						
Dataset	s	Ours	Ours-U	PT-FedAvg	pFedHN	Fed-DualPrompt	FedMoon	FedMix
CIFAR-100	10	81.09 (0.40)	82.45 (0.39)	78.29 (1.46)	76.86 (0.95)	78.91 (0.93)	79.39 (0.53)	80.23 (0.40)
	5	<u>78.32 (0.35)</u>	80.15 (0.14)	72.44 (3.52)	72.62 (2.73)	73.51 (2.97)	74.80 (3.17)	75.51 (1.81)
CIFAR-100-C	10	70.89 (0.26)	71.84 (0.25)	69.73 (0.25)	70.41 (0.17)	70.26 (0.18)	69.56 (0.31)	<u>71.01 (0.17)</u>
	2	<u>62.42 (4.10)</u>	63.77 (4.22)	60.69 (9.84)	56.60 (9.87)	59.53 (5.35)	58.23 (9.98)	61.47 (8.44)
Five-Dataset	-	79.31 (1.75)	-	77.82 (23.17)	78.00 (0.12)	<u>78.97 (3.36)</u>	<u>77.52 (2.23)</u>	77.62 (3.56)

Algorithm 1 FGPT Training Algorithm

Server Input: initial weights $W = \{W_C, P_G, P_S\}$, Number of participating clients in each round $m = \gamma \times M$, number of communication rounds T , client data ratio set $\{\alpha_i\}_{i=1}^M$, group frequencies $\{\beta_g^i\}_{i=1}^M, g \in [G]$.

Client i 's Input: Pre-trained Transformer h_θ , Prompt Selection module $Select$ with orthogonal keys $B = \{b_g\}_{g=1}^G$, training data $(x_i, y_i) \sim D_i$ for client i , learning rate η , number of local training steps E .

- 1: For $t = 1 \rightarrow T$ rounds, sample m clients and execute **Procedure A** and **Procedure C** iteratively.
- 2: **procedure A:** CLIENTUPDATE(i)
- 3: $W_i \leftarrow W$ ▷ Initialize with global model
- 4: **for** $e = 1 \rightarrow E$ **do**
- 5: With local client data $(x_i^{e,t}, y_i^{e,t})$ execute
- 6: PROMPTSELECTION to select prompt p_g for each sample,
- 7: $W_i \leftarrow W_i - \eta \cdot \nabla l(p_g, P_S, W_C; x_i^{e,t}, y_i^{e,t})$ ▷ SGD update based on objective (1)
- 8: **end for**
- 9: Send W_i to SERVEREXECUTE
- 10: **end procedure**
- 11: **procedure B:** PROMPTSELECTION($Select, x, y$)
- 12: $g \leftarrow Select(x)$ ▷ Obtain group ID
- 13: $p_g \leftarrow P_{Select(x)}$ ▷ Select corresponding group prompt
- 14: **end procedure**
- 15: **procedure C:** SERVEREXECUTE(t)
- 16: receive local models’ weights $\{W_i\}_{i=1}^m$ from CLIENTUPDATE
- 17: $[W_C, P_S] \leftarrow \sum_{i=1}^m \alpha_i [W_C^i, P_S^i]$ ▷ Aggregation
- 18: **for** $g = 1 \rightarrow G$ **do**
- 19: $p_g \leftarrow \sum_{i=1}^m \beta_g^i p_g^i$ ▷ Group Aggregation
- 20: **end for**
- 21: broadcast W to CLIENTUPDATE
- 22: **end procedure**

similar group prompts, and then each chosen prompt is used independently to obtain its prediction logit. Finally, the logits are averaged to make the final prediction. Details of FGPT-U are shown in the Appendix (Algorithm 3). The results presented in Table 1 serve as concrete evidence that employing ensemble predictions leads to additional enhancements in performance. It is notable that we can use a lighter-weighted encoder (*i.e.*, ResNet) in the prompt selection module to improve efficiency, we also report the results in Appendix.

Algorithm 2 FGPT Inference Algorithm.

Input: Pre-trained Transformer h_θ with U layers, layer u to insert group prompts, trainable weights $W = \{W_C, P_G, P_S\}$, Prompt Selection Module $Select$ with orthogonal keys $B = \{b_g\}_{g=1}^G$, a single test sample x_n .

- 1: Extract representation $h_\theta(x_n)$ with pre-trained model h_θ
- 2: $g \leftarrow \arg \max_{g \in G} \cos(h_\theta(x_n), b_g)$ ▷ Obtain group ID
- 3: Select corresponding group prompt p_g
- 4: Encode x_n into \mathbf{E}_0 ▷ Encode image into patch embedding (Section 2.2)
- 5: **for** $i = 1 \rightarrow U$ **do**
- 6: **if** $i = 1$ **then**
- 7: $[\text{cls}_1, \mathbf{Z}_1^S, \mathbf{E}_1] = h_\theta^{(1)}([\text{cls}_0, P_S, \mathbf{E}_0])$. ▷ Insert shared prompts
- 8: **else if** $i < u$ **then**
- 9: $[\text{cls}_i, \mathbf{Z}_i^S, \mathbf{E}_i] = h_\theta^{(i)}([\text{cls}_{i-1}, \mathbf{Z}_{i-1}^S, \mathbf{E}_{i-1}])$.
- 10: **else if** $i = u$ **then**
- 11: $[\text{cls}_u, \mathbf{Z}_u^g, \mathbf{Z}_u^S, \mathbf{E}_u] =$
- 12: $h_\theta^{(u)}([\text{cls}_{u-1}, p_g, \mathbf{Z}_{u-1}^S, \mathbf{E}_{u-1}])$. ▷ Insert group prompt
- 13: **else**
- 14: $[\text{cls}_i, \mathbf{Z}_i^g, \mathbf{Z}_i^S, \mathbf{E}_i] =$
- 15: $h_\theta^{(i)}([\text{cls}_{i-1}, \mathbf{Z}_{i-1}^g, \mathbf{Z}_{i-1}^S, \mathbf{E}_{i-1}])$.
- 16: **end if**
- 17: **end for**
- 18: $y^* \leftarrow f(W_C, \text{cls}_U)$ ▷ Final Prediction
- 19: **return** final logits prediction y^*

4 Experiments

4.1 Experimental setup

Datasets

We demonstrate the effectiveness of our proposed approach using three datasets: (1) *CIFAR100 dataset*. Following the evaluation in [24], we use CIFAR100 which comprises 50,000 training images and 10,000 testing images distributed across 100 classes. (2) *CIFAR100-C* [9] augments CIFAR100 with different visual corruptions, we take the first 10 domains and random sample 1000 images from each domain and got 10000 images spanning 100 classes. (3) *Fivedataset* consists of a sequence of 5 datasets (SVHN, CIFAR10, not-MNIST, Fashion-MNIST, and MNIST) as outlined in the work by [7]. These datasets present smaller inter-dataset similarities across different tasks, thus introducing a heavier heterogeneity. To elaborate, we randomly select 1000 samples from each dataset and divide them into training and test sets.

Non-IID Setting

In this section, we introduce the FL environments and data partition strategies for different datasets. For CIFAR-100, we introduce 100 clients and set the client participating ratio (γ) to 0.05. For CIFAR-100-C, we introduce 50 clients and set the client participating ratio (γ) to 0.1. For CIFAR-100 and CIFAR-100-C, to introduce data heterogeneity among clients, we applied the ‘‘Pathological Partition’’ [24, 16] split strategy to simulate non-IID scenarios.² We first sort the data by labels and then allocate data from a specific number of classes (s) to each client. Since s is related to the maximum number of classes each user can have, as s decreases, the degree of data heterogeneity increases. As to the Fivedatasets, we evenly distribute the data among 20 clients, with every 4 clients originating from the same dataset. We set the participating rate $\gamma = 0.1$, and perform training for 60 communication rounds.

Implementation Details

We use ViT-B-16 [6] as our model, which is originally trained on images with size 224 and patch size 16. Consequently, we resized our images to 224 to align with the model’s specifications. The ViT-B-16 model was pre-trained on ImageNet-21K due to its small domain gap with CIFAR100. During the prompt-tuning process, we focused on the shared prompts, group prompts, and the classifier. We used local training epochs $E = 5$ for all experiments. For shared prompts, we follow the design of VPT-shallow [11] and set the prompt length as 5 for efficiency. For group prompts, we append prompts to the 6-th layer and set the group prompt length as 1 for efficiency. The group number varies under different heterogeneities which we studied in Table 4.

4.2 Comparison with Baselines

We conducted a comparative analysis of our method against various global-model approaches: visual prompt-tuning [11] that optimized using FedAvg [23], recent FedMoon [17] and FedMix [37]. Additionally, for personalized FL, we considered pFedHN [16, 29] as this method learns a global Hyper-Network to produce personalized parameters³. In addition, we combine the continual learning method [35, 34] with FedAvg as a strong baseline, denoted as Fed-DualPrompt. To ensure a fair comparison, we implemented the baseline methods using the visual prompt-tuning approach. Specifically, for global-model approaches, all parameters were shared during the learning process. We fine-tuned the hyperparameters to obtain the best performance for each of the baseline methods.

Average Performance of Models

During each communication round, we evaluate the performance of each model on a local test dataset that was not used during training. We calculate *Accuracy* which represents the ratio of correct predictions made over the total number of testing images. To ensure robust evaluation, we consider the evaluation results from the last 10 communication rounds. From these results, we compute the mean test accuracy and variance for comparison. The

²We also report results with ‘‘Dirichlet Partition’’ in Table 7 in the Appendix.

³It is worth mentioning that it is not easy to adapt the existing finetuning-based and clustering-based PFL methods to align with our comparison, where our primary focus is training a single FL model that can be generalizable, even on unseen clients without the need for additional expensive fine-tuning. Besides, these methods are restricted by their efficiency compared with prompt tuning, *e.g.*, personalizing different parts of the model and linearly increasing complexity with client counts [22], especially when adapting to Transformer.

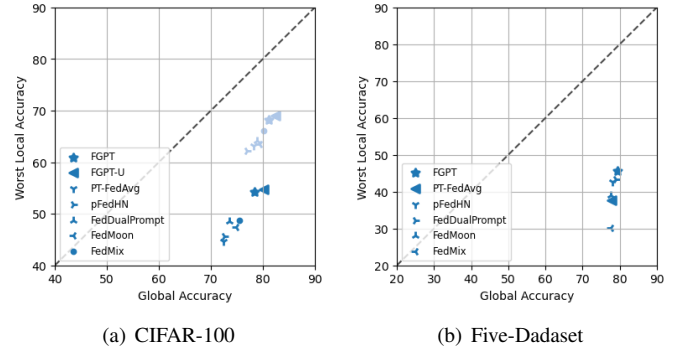


Figure 2: Global accuracy and worst local accuracy on (a) CIFAR-100, and (b) Five-Dataset. The grey and blue markers correspond to $s = 10$ and $s = 5$ classes, respectively. Points located in the top-right corner correspond to improved performance on both the global data and local clients’ data distributions. Our proposed FGPT (\star) and FGPT-U (\triangle) achieves the superior performance compared with baselines.

results on CIFAR-100 and CIFAR-100-C datasets are presented in Table 1. It can be observed that FGPT consistently achieves a better accuracy across various degrees of data heterogeneity and various datasets in most cases. With the help of ensemble prediction, FGPT-U further improves the results. Although FedMix [37] performs well in some cases, it requires the sharing of additional information (averaged images) for training. It is worth noting that Prompt-Tuning with FedAvg serves as a strong baseline which is comparable to recent FL algorithms. This can be attributed to the effectiveness of Transformer in mitigating catastrophic forgetting, accelerating convergence, and achieving superior global models, particularly when dealing with heterogeneous data [25]. The results on Fivedataset are also presented in Table 1 and we only report the results from FGPT since we set the group number as 5, FGPT outperforms baseline methods on Fivedataset.

Global and Local Performance Trade-off

We demonstrate our method’s capacity to achieve high test accuracy on both the global data distribution and the local clients’ data distributions. As shown in Figure 2, we visualize both the accuracy (denoted as global accuracy in the figure) and the worst local accuracy (client with the worst test accuracy). Figure 2 (a) illustrates the results on the CIFAR-100 dataset, the grey and blue markers represent $s = 10$ and $s = 5$, respectively. Figure 2 (b) illustrates the results on the Five-Dataset. Points situated in the top-right corner indicate better performance in both global data distribution and local clients’ data distribution. Notably, our method exhibits the greatest ability to align with both global and local data distributions.

Efficiency

In this section, we conduct a comparison between the number of parameters that need training and communication between FGPT and training a whole network in classical FL (*e.g.*, FedAvg [23]). As shown in Table 2, prompt-tuning requires significantly smaller trainable parameters thus improving the efficiency and saving the communication cost a lot. We also analyze the efficiency of different methods in Section D.3 in Appendix.

Table 2: Training and Communication Cost. The FedAvg trains the whole model, we show the number of parameters that need updating and communication with different architectures like ResNet and ViT. Compared with our method FGPT, traditional methods needs heavy parameter update and communication architectures.

Method	FedAvg			Ours
	ResNet-18	ResNet-50	ViT-16/B	ViT-16/B
# Parameters ↓	11M	24M	86M	0.1M

Table 3: Varying the number of groups under various heterogeneity scenarios.

Num. of Groups $\gamma = 0.05$	Performance ↑	
	$E = 5, s = 10$	$E = 5, s = 5$
15	80.30 (0.74)	77.30 (0.52)
20	81.09 (0.40)	78.25 (0.40)
25	80.80 (0.16)	78.32 (0.35)
30	80.43 (0.01)	77.48 (0.32)
35	79.21 (0.42)	76.59 (0.75)

Table 4: Ablation studies with different improvements. We report the results on the CIFAR-100 dataset with $s = 10$.

PT-FedAvg	Group Prompt	Orthogonal Key	U-inference	Accuracy ↑
✓				78.29
✓	✓			80.56
✓	✓	✓		81.09
✓	✓	✓	✓	82.45

4.3 Ablation Studies

Effect of Heterogeneity

Data heterogeneity represents a critical challenge in FL. To assess the influence of data heterogeneity on the performance of various methods, we conducted experiments with varying degrees of heterogeneity. Specifically, we introduced significant label heterogeneity by setting the Pathological partition parameter s to values of 5 and 10. The results are presented in Table 1. It is evident that as the degree of data heterogeneity increases (with a smaller value of s), the performance of all methods decreases. However, our methods consistently outperforms the others and demonstrates robustness to label distribution heterogeneity.

The Effect of Number of Groups

In this section, we delve into the relationship between the number of groups, which varies from 15 to 35, and the level of heterogeneity, aiming to determine the optimal group number for different heterogeneity settings. The results are summarized in Table 3, indicating that as we increase the level of heterogeneity (by decreasing s from 10 to 5), the optimal group number also tends to increase (from 20 to 25) to yield the best results. This finding aligns with our analysis presented in Theorem 5.1, which suggests that higher heterogeneity leads to a greater distribution mismatch and by increasing the number of groups, we can mitigate this mismatch and strike a favorable balance between generalization and distribution matching.

The Effect of Orthogonal Key

In this section, we analyze the impact of orthogonally initialized keys by comparing their test performance with randomly initialized keys. The results, presented in Table 4, demonstrate that

using orthogonal keys improved the accuracy by 0.53% compared to random keys on the CIFAR-100 dataset when $s = 10$ and $E = 5$.

The Effect of U-Inference

Theorem 5.1 illustrates the trade-off between generalization and distribution matching. In order to enhance the generalization ability of FGPT, we proposed the U-inference method to effectively address this concern. By selecting and ensembling the Top-K most relevant prompts for prediction, the prediction accuracy significantly improved. As shown in Table 4, the U-inference yields an increase of approximately 1.5% on CIFAR-100 dataset with $s = 10$. In addition, Table 1 and Table 7 in Appendix all demonstrate significant performance improvement with U-inference, providing strong evidence of the efficacy of FGPT-U. It is notable we further analyzed the efficiency of U-Inference in the Appendix.

5 Theoretical Insights

Our aim in this section is to provide analytical justification for the role of group prompts in narrowing the empirical risk of the global model found by empirical loss minimization and the population risk of the optimal model of a client. For simplicity, we focus here on group prompts.

5.1 Theoretical Results

We start with some general notation and definitions used throughout the theory. We assume that the global data distribution \mathcal{D} can be categorized into G distinct groups. For example, this is accomplished using the *Select* function as shown in Eq. 5. With this, let \mathcal{D}_g^i denote the distribution of data from the g -th group of client i . Thus, the participated clients' data distribution [10, 39] for the g -th group is:

$$\mathcal{C}_g = \sum_{i=1}^M \pi_g^i \mathcal{D}_g^i \quad (6)$$

where $\pi_g^i = \frac{N_g^i}{N_i}$ is the probability of a data sample on client i belong to group g and N_g^i is a fixed number of samples from \mathcal{D}_g^i for all $g \in [G], i \in [M]$, and $N_g \triangleq \sum_{g \in [G]} N_g^i$. We then define \mathcal{C}_g and $\hat{\mathcal{C}}_g$ as the population and empirical distributions, respectively, of data group g . Finally, for $g \in [G]$ and hypothesis $h_g \in \mathcal{H}$, we use $h_{Select} = \{h_1, \dots, h_g, \dots, h_G\}_{Select(x)}$ to denote the group-aware hypothesis determined by *Select* when datapoint x is given as input. Let $\hat{h}_g = \arg \min_{h \in \mathcal{H}} \mathcal{L}_{\hat{\mathcal{C}}_g}(h)$ denote the empirical model for data group g and $\hat{h}_{Select} = \{\hat{h}_1, \dots, \hat{h}_g, \dots, \hat{h}_G\}_{Select(x)}$ denote the corresponding global model. With this notation, we have the following result. Please see the appendix for further details on notation and the proof.

Theorem 5.1 (Gap between the global and local performance.). *Assume the loss function ℓ is bounded in $[0, 1]$ and the function *Select* is a data grouping method. Let $\mathfrak{R}_{\mathcal{D}, m}(\mathcal{H})$ represent the Rademacher complexity of the hypothesis class \mathcal{H} over the distribution \mathcal{D} with m samples. Then, with a probability of at least*

$1 - \delta$ over the training set,

$$\begin{aligned} & \mathcal{L}_{\widehat{\mathcal{D}}_i}(\widehat{h}_{\text{Select}}) - \min_{h \in \mathcal{H}} \mathcal{L}_{\mathcal{D}_i}(h) \\ & \leq \sqrt{\frac{\log \frac{1}{\delta}}{N_i}} + 2 \sum_{i=1}^G \frac{N_g^i}{N_i} \mathfrak{R}_{\mathcal{C}_g, N_g}(\mathcal{H}) \\ & \quad + \sum_{g=1}^G \frac{N_g^i}{N_i} \left(\text{disc}(\mathcal{D}_g^i, \mathcal{C}_g) + \text{disc}(\widehat{\mathcal{D}}_g^i, \widehat{\mathcal{C}}_g) \right), \end{aligned} \quad (7)$$

where $\text{disc}_{\mathcal{H}}(\mathcal{D}_1, \mathcal{D}_2) = \max_{h \in \mathcal{H}} |\mathcal{L}_{\mathcal{D}_1}(h) - \mathcal{L}_{\mathcal{D}_2}(h)|$.

The left-hand side of Eq.7 represents the gap between the minimum empirical risk⁴. of the global model found by empirical loss minimization using the `select` grouping function and the population loss of the optimal model of client i . The right-hand side of Eq.7 bounds this gap with respect to weighted averages, with weights proportional to N_g^i , of the Rademacher complexity of group distributions and discrepancy measures between the global group distribution \mathcal{C}_g and the local group distribution \mathcal{D}_g^i of client i . To interpret this, consider the effect of an increased number of groups G with fixed total number of data N . As G increases, the Rademacher complexity term increases because $N_g \propto N/G$ decreases. On the other hand, the discrepancy term decreases because data within the same group become more similar. This tradeoff suggests that tuning G is important in achieving optimal performance. This agrees with our experiments in Table 3.

6 Conclusion

In this paper, we introduce a new heterogeneous FL methods for Transformers with prompt-tuning, called `FGPT`, which learns a single global model that can achieve good test accuracy on both global data and local clients' data distributions. `FGPT` utilizes shared prompts and group prompts to facilitate the learning of both universal and group-specific knowledge. The prompt selection module assigns each input a specific group prompt, enabling sample-level personalization and fostering collaboration among data from the same group across different clients. An important advantage of `FGPT` is its ability to be directly applied to new clients, as it personalizes every input sample and achieves efficiency by requiring only one additional inference during prompt selection. Additionally, a test time ensemble variant `FGPT-U` is proposed to further enhance the model's generalization ability. Through extensive experiments, we show `FGPT` and `FGPT-U` can significantly outperform the baseline methods under different settings on image classification tasks with ViTs. Encouraged by the superior performance of our algorithm in vision tasks, in future work we will explore the effectiveness of `FGPT` on natural language processing tasks using Transformer-based large language models.

7 Acknowledgements

This work is supported in part by the Natural Sciences and Engineering Research Council of Canada (NSERC), in part by NSERC Discovery Grant RGPIN-2021-03677, and in part by NVIDIA Hardware Award.

⁴It is notable we also give the gap on population distribution in Section C.4 in Appendix

References

- [1] Bao, W., Wang, H., Wu, J., He, J.: Optimizing the collaboration structure in cross-silo federated learning. arXiv preprint arXiv:2306.06508 (2023)
- [2] Bhojanapalli, S., Chakrabarti, A., Glasner, D., Li, D., Unterthiner, T., Veit, A.: Understanding robustness of transformers for image classification. In: Proceedings of the IEEE/CVF international conference on computer vision. pp. 10231–10241 (2021)
- [3] Caldarola, D., Mancini, M., Galasso, F., Ciccone, M., Rodolà, E., Caputo, B.: Cluster-driven graph federated learning over multiple domains. In: Proceedings of the IEEE/CVF Conference on Computer Vision and Pattern Recognition. pp. 2749–2758 (2021)
- [4] Chen, H.Y., Chao, W.L.: Fedbe: Making bayesian model ensemble applicable to federated learning. arXiv preprint arXiv:2009.01974 (2020)
- [5] Dong, B., Zhou, P., Yan, S., Zuo, W.: Lpt: Long-tailed prompt tuning for image classification. arXiv preprint arXiv:2210.01033 (2022)
- [6] Dosovitskiy, A., Beyer, L., Kolesnikov, A., Weissenborn, D., Zhai, X., Unterthiner, T., Dehghani, M., Minderer, M., Heigold, G., Gelly, S., et al.: An image is worth 16x16 words: Transformers for image recognition at scale. arXiv preprint arXiv:2010.11929 (2020)
- [7] Ebrahimi, S., Meier, F., Calandra, R., Darrell, T., Rohrbach, M.: Adversarial continual learning. In: Computer Vision—ECCV 2020: 16th European Conference, Glasgow, UK, August 23–28, 2020, Proceedings, Part XI 16. pp. 386–402. Springer (2020)
- [8] Ghosh, A., Chung, J., Yin, D., Ramchandran, K.: An efficient framework for clustered federated learning. Advances in Neural Information Processing Systems **33**, 19586–19597 (2020)
- [9] Hendrycks, D., Dietterich, T.G.: Benchmarking neural network robustness to common corruptions and surface variations. arXiv preprint arXiv:1807.01697 (2018)
- [10] Hu, X., Li, S., Liu, Y.: Generalization bounds for federated learning: Fast rates, unparticipating clients and unbounded losses. In: The Eleventh International Conference on Learning Representations (2023)
- [11] Jia, M., Tang, L., Chen, B.C., Cardie, C., Belongie, S., Hariharan, B., Lim, S.N.: Visual prompt tuning. In: Computer Vision—ECCV 2022: 17th European Conference, Tel Aviv, Israel, October 23–27, 2022, Proceedings, Part XXXIII. pp. 709–727. Springer (2022)
- [12] Karimireddy, S.P., Jaggi, M., Kale, S., Mohri, M., Reddi, S.J., Stich, S.U., Suresh, A.T.: Mime: Mimicking centralized stochastic algorithms in federated learning. arXiv preprint arXiv:2008.03606 (2020)
- [13] Karimireddy, S.P., Kale, S., Mohri, M., Reddi, S., Stich, S., Suresh, A.T.: Scaffold: Stochastic controlled averaging for federated learning. In: International Conference on Machine Learning. pp. 5132–5143. PMLR (2020)

- [14] Khan, S., Naseer, M., Hayat, M., Zamir, S.W., Khan, F.S., Shah, M.: Transformers in vision: A survey. *ACM computing surveys (CSUR)* **54**(10s), 1–41 (2022)
- [15] Kulkarni, V., Kulkarni, M., Pant, A.: Survey of personalization techniques for federated learning. In: 2020 Fourth World Conference on Smart Trends in Systems, Security and Sustainability (WorldS4). pp. 794–797. IEEE (2020)
- [16] Li, H., Cai, Z., Wang, J., Tang, J., Ding, W., Lin, C.T., Shi, Y.: Fedtp: Federated learning by transformer personalization. *arXiv preprint arXiv:2211.01572* (2022)
- [17] Li, Q., He, B., Song, D.: Model-contrastive federated learning. In: Proceedings of the IEEE/CVF conference on computer vision and pattern recognition. pp. 10713–10722 (2021)
- [18] Li, T., Sahu, A.K., Zaheer, M., Sanjabi, M., Talwalkar, A., Smith, V.: Federated optimization in heterogeneous networks. *Proceedings of Machine learning and systems* **2**, 429–450 (2020)
- [19] Li, T., Sahu, A.K., Zaheer, M., Sanjabi, M., Talwalkar, A., Smith, V.: Feddane: A federated newton-type method. In: 2019 53rd Asilomar Conference on Signals, Systems, and Computers. pp. 1227–1231. IEEE (2019)
- [20] Li, X., Jiang, M., Zhang, X., Kamp, M., Dou, Q.: Fedbn: Federated learning on non-iid features via local batch normalization. *arXiv preprint arXiv:2102.07623* (2021)
- [21] Mansour, Y., Mohri, M., Ro, J., Suresh, A.T.: Three approaches for personalization with applications to federated learning. *arXiv preprint arXiv:2002.10619* (2020)
- [22] Marfoq, O., Neglia, G., Bellet, A., Kameni, L., Vidal, R.: Federated multi-task learning under a mixture of distributions. *Advances in Neural Information Processing Systems* **34**, 15434–15447 (2021)
- [23] McMahan, B., Moore, E., Ramage, D., Hampson, S., y Arcas, B.A.: Communication-efficient learning of deep networks from decentralized data. In: Artificial intelligence and statistics. pp. 1273–1282. PMLR (2017)
- [24] Oh, J., Kim, S., Yun, S.Y.: Fedbabu: Towards enhanced representation for federated image classification. *arXiv preprint arXiv:2106.06042* (2021)
- [25] Qu, L., Zhou, Y., Liang, P.P., Xia, Y., Wang, F., Adeli, E., Fei-Fei, L., Rubin, D.: Rethinking architecture design for tackling data heterogeneity in federated learning. In: Proceedings of the IEEE/CVF Conference on Computer Vision and Pattern Recognition. pp. 10061–10071 (2022)
- [26] Raghu, M., Unterthiner, T., Kornblith, S., Zhang, C., Doso-vitskiy, A.: Do vision transformers see like convolutional neural networks? *Advances in Neural Information Processing Systems* **34**, 12116–12128 (2021)
- [27] Reddi, S., Charles, Z., Zaheer, M., Garrett, Z., Rush, K., Konečný, J., Kumar, S., McMahan, H.B.: Adaptive federated optimization. *arXiv preprint arXiv:2003.00295* (2020)
- [28] Ruan, Y., Joe-Wong, C.: Fedsoft: Soft clustered federated learning with proximal local updating. In: Proceedings of the AAAI Conference on Artificial Intelligence. vol. 36, pp. 8124–8131 (2022)
- [29] Shamsian, A., Navon, A., Fetaya, E., Chechik, G.: Personalized federated learning using hypernetworks. In: International Conference on Machine Learning. pp. 9489–9502. PMLR (2021)
- [30] Shi, N., Lai, F., Kontar, R.A., Chowdhury, M.: Fed-ensemble: Improving generalization through model ensembling in federated learning. *arXiv preprint arXiv:2107.10663* (2021)
- [31] Singhal, K., Sidahmed, H., Garrett, Z., Wu, S., Rush, J., Prakash, S.: Federated reconstruction: Partially local federated learning. *Advances in Neural Information Processing Systems* **34**, 11220–11232 (2021)
- [32] Vaswani, A., Shazeer, N., Parmar, N., Uszkoreit, J., Jones, L., Gomez, A.N., Kaiser, Ł., Polosukhin, I.: Attention is all you need. *Advances in neural information processing systems* **30** (2017)
- [33] Wang, H., Yurochkin, M., Sun, Y., Papailiopoulos, D., Khazaeni, Y.: Federated learning with matched averaging. *arXiv preprint arXiv:2002.06440* (2020)
- [34] Wang, Z., Zhang, Z., Ebrahimi, S., Sun, R., Zhang, H., Lee, C.Y., Ren, X., Su, G., Perot, V., Dy, J., et al.: Dual-prompt: Complementary prompting for rehearsal-free continual learning. In: Computer Vision–ECCV 2022: 17th European Conference, Tel Aviv, Israel, October 23–27, 2022, Proceedings, Part XXVI. pp. 631–648. Springer (2022)
- [35] Wang, Z., Zhang, Z., Lee, C.Y., Zhang, H., Sun, R., Ren, X., Su, G., Perot, V., Dy, J., Pfister, T.: Learning to prompt for continual learning. In: Proceedings of the IEEE/CVF Conference on Computer Vision and Pattern Recognition. pp. 139–149 (2022)
- [36] Wu, S., Li, T., Charles, Z., Xiao, Y., Liu, Z., Xu, Z., Smith, V.: Motley: Benchmarking heterogeneity and personalization in federated learning. *arXiv preprint arXiv:2206.09262* (2022)
- [37] Yoon, T., Shin, S., Hwang, S.J., Yang, E.: Fedmix: Approximation of mixup under mean augmented federated learning. *arXiv preprint arXiv:2107.00233* (2021)
- [38] Yu, Y., Wei, A., Karimireddy, S.P., Ma, Y., Jordan, M.: Tct: Convexifying federated learning using bootstrapped neural tangent kernels. *Advances in Neural Information Processing Systems* **35**, 30882–30897 (2022)
- [39] Yuan, H., Morningstar, W., Ning, L., Singhal, K.: What do we mean by generalization in federated learning? *arXiv preprint arXiv:2110.14216* (2021)
- [40] Yurochkin, M., Agarwal, M., Ghosh, S., Greenewald, K., Hoang, N., Khazaeni, Y.: Bayesian nonparametric federated learning of neural networks. In: International conference on machine learning. pp. 7252–7261. PMLR (2019)
- [41] Zhou, Y., Pu, G., Ma, X., Li, X., Wu, D.: Distilled one-shot federated learning. *arXiv preprint arXiv:2009.07999* (2020)

Overall pipeline of Appendix. We first introduce related work in Section A. Then the algorithm details of FGPT-U and its analysis are explained in Section B. In Section C, we introduce the proof of Theorem 5.1 along with required lemmas. Finally, additional experiments are reported in Section D for a more comprehensive study.

A Related Work

A.1 Generic Federated Learning

FedAvg [23] is a standard FL algorithm that involves multiple rounds of local training and global aggregation. Many works focus on improving FedAvg through various aspects: (1) global aggregation methods [33, 40, 4, 41] replace the weight average with more dedicated strategies like ensemble and distillation. (2) optimization methods [13, 18, 12] reduce the client drifts [13] by correcting local gradients [13] or employed regularization toward the global model [18, 19] thus achieving a better convergence rate.

A.2 Personalized Federated Learning

PFL [15] learns a customized model for each client. To be specific, Fine-tuning methods [31, 24] adjust a global or meta-trained model to adapt to local client data by fine-tuning part of the global model. Clustered FL [8, 21, 3] clusters clients with similar data distribution, assuming that they can share the same optimal model, however, imposes a heavy computational burden. pFedHN [29] learns a hypernetwork at the server to aggregate clients’ model updates and produce their entire models for the next round. The disadvantage of PFL is overcoming challenges in adapting to new clients and overfitting local data. In this paper, we learn a uniform FL model that not only achieves high accuracy on the global distribution but is also capable of aligning with different local distributions without local adaptation.

B Algorithm details

B.1 Notation

For convenience, we summarize the notations used in this paper in Table 5.

B.2 FGPT-U Details

Tesing phase of FGPT-U.

We illustrate the inference procedure of FGPT-U in Algorithm 3, FGPT-U differs from FGPT only during the inference stage, in that it utilizes more group prompts for predictions. Specifically, we select the top- K (in our case, $K = 5$) group prompts and ensemble their results. As shown in line 12 of Algorithm 3, each chosen prompt is used independently for inference, and the logits obtained from each prompt are averaged to make the final prediction. We also mark the difference between FGPT-U and FGPT with **diff** in Algorithm 3. It is worth noting that the computational cost remains relatively low as the features before the group prompt layer only infer once.

Table 5: Main notations used in this paper.

Basic Variables	
M	\triangleq Number of clients
\mathcal{X}	\triangleq Input space
\mathcal{Y}	\triangleq Label space
\mathcal{D}_i	\triangleq Data distribution on client i and \mathcal{D}_i is on $\mathcal{X} \times \mathcal{Y}$
$N = \sum_{i=1}^M N_i$	\triangleq N_i is number of data samples at client i and N is the number of data on all clients
$\{x_i, y_i\} \sim \mathcal{D}_i$	\triangleq Data sample (x_i, y_i) located on participating client i is made of i.i.d sampling from \mathcal{D}_i .
Function Variables	
ℓ	\triangleq loss function
$Select$	\triangleq Prompt Selection function
\mathcal{G}, G	\triangleq Group set, number of groups $ \mathcal{G} $
\mathcal{D}_g^i	\triangleq Data distribution on client i from group g
N_g^i	\triangleq Number of data samples at client i from group g
$N_g = \sum_{i=1}^M N_g^i$	\triangleq Number of data samples from group g
\mathcal{B}, b_g	\triangleq Keys set, key of g -th group $ \mathcal{G} $
P_G	\triangleq Weight of group prompts
P_S	\triangleq Weight of shared prompts
W_C	\triangleq Weight of classifier
h_θ	\triangleq Pretrained foundation model
cls	\triangleq Classification token
\mathbf{E}	\triangleq Image patch embeddings
\mathbf{Z}	\triangleq Prompt features embeddings

Table 6: U-Inference Ablation, $U = K$ means take the top- K prompts for inference. We can see with $U = 2$ will bring the major improvements.

FL settings		Accuracy		
dataset	s	Ours	U=2	U=5
CIFAR-100	10	81.09 (0.40)	82.13 (0.39)	82.45 (0.41)
CIFAR-100-C	10	70.89 (0.26)	71.51 (0.38)	71.84 (0.25)

Advantage of FGPT-U.

According to Theorem 5.1, increasing the number of groups, denoted as G , leads to a decrease in generalization. In light of this, FGPT-U is proposed to enhance the group-specific parameters by ensembling them during inference for a better generalization [30]. The performance outcomes, as presented in Table 1 and Table 7, demonstrate the efficacy of ensembling the group prompts. FGPT-U significantly improves the performance of FGPT by a substantial margin (more than 1% on average).

Efficiency of U-inference

It is important to note that the computational cost remains relatively low since the group prompts’ layer is positioned at a relatively high level in our approach. This positioning only requires multiple inferences at the later layers, thus helping to ensure efficient processing despite the ensemble nature of the U-inference procedure. Also, we wish to emphasize that using the Top-2 prompt for inference will directly bring major improvements, the results on CIFAR-100 and CIFAR-100-C with $E = 5$ are shown in Table 6.

Algorithm 3 FGPT-U Inference Algorithm.

Input: Pre-trained Transformer h_θ with U layers, layer u to insert group prompts, trainable weights $W = \{W_C, P_G, P_S\}$, cluster function *Select* with orthogonal keys $B = \{b_g\}_{g=1}^G$, a single test sample x_n , K Number of prompts to choose.

- 1: Extract representation $h_\theta(x_n)$ with pre-trained model h_θ
- 2: $I \leftarrow \arg \max_{I \subset [G]: |I|=K} \sum_{g \in I} \cos(h_\theta(x_n), b_g)$ \triangleright Obtain top- K group IDs (**diff**)
- 3: $P_I = \{p_g\}_{g \in I}$ \triangleright Select corresponding group prompt
- 4: Encode x_n into \mathbf{E}_0 \triangleright Encode image into patch embedding (Section 2.2)
- 5: **for** $i = 1 \rightarrow u$ **do**
- 6: **if** $i = 1$ **then**
- 7: $[\mathbf{cls}_1, \mathbf{Z}_1^S, \mathbf{E}_1] = h_\theta^{(1)}([\mathbf{cls}_0, P_S, \mathbf{E}_0])$. \triangleright Insert shared prompts
- 8: **else**
- 9: $[\mathbf{cls}_i, \mathbf{Z}_i^S, \mathbf{E}_i] = h_\theta^{(i)}([\mathbf{cls}_{i-1}, \mathbf{Z}_{i-1}^S, \mathbf{E}_{i-1}])$.
- 10: **end if**
- 11: **end for**
- 12: **for** $p_g \in P_I$ **do** \triangleright (**diff**)
- 13: **for** $i = u \rightarrow U$ **do**
- 14: **if** $i = u$ **then**
- 15: $[\mathbf{cls}_u^g, Z_u^g, \mathbf{Z}_u^{S,g}, \mathbf{E}_u^g] =$
- 16: $h_\theta^{(u)}([\mathbf{cls}_{u-1}, p_g, \mathbf{Z}_{u-1}^S, \mathbf{E}_{u-1}])$. \triangleright Insert group prompt
- 17: **else**
- 18: $[\mathbf{cls}_i^g, Z_i^g, \mathbf{Z}_i^{S,g}, \mathbf{E}_i^g] =$
- 19: $h_\theta^{(i)}([\mathbf{cls}_{i-1}^g, Z_{i-1}^g, \mathbf{Z}_{i-1}^{S,g}, \mathbf{E}_{i-1}^g])$.
- 20: **end if**
- 21: **end for**
- 22: $y_g^* \leftarrow f(W_C, \mathbf{cls}_U^g)$
- 23: **end for**
- 24: $y^* \leftarrow \text{mean}(\{y_g^*\}_{g \in I})$ \triangleright Final Prediction (**diff**)
- 25: **return** final logits prediction y^*

C Technical details and Omitted proofs

C.1 Settings and Definitions

First, we formally set up some general notation: For a distribution \mathcal{P} with support $(\mathcal{X}, \mathcal{Y})$ and a non-negative loss function $\ell: \mathcal{X} \times \mathcal{Y} \rightarrow \mathbb{R}^+$ denote the population risk of a hypothesis $h: \mathcal{X} \rightarrow \mathcal{Y}$ as follows:

$$\mathcal{L}_{\mathcal{P}}(h) = \mathbb{E}_{(X,Y) \sim \mathcal{P}}[\ell(h(X), Y)].$$

Let \mathcal{H} represent a hypothesis class and denote the hypothesis \hat{h} minimizing the empirical risk as

$$\hat{h} = \arg \min_{h \in \mathcal{H}} \mathcal{L}_{\hat{\mathcal{P}}}(h),$$

where we denote $\hat{\mathcal{P}}$ the empirical distribution of samples drawn iid from \mathcal{P} . We will also denote $\mathfrak{R}_{\mathcal{P}, m}(\mathcal{H})$ the Rademacher complexity of the hypothesis class \mathcal{H} over the distribution \mathcal{P} with m samples. Furthermore, we define the distribution mismatch between two distributions \mathcal{P}_1 and \mathcal{P}_2 as

$$\text{disc}_{\mathcal{H}}(\mathcal{P}_1, \mathcal{P}_2) = \max_{h \in \mathcal{H}} |\mathcal{L}_{\mathcal{P}_1}(h) - \mathcal{L}_{\mathcal{P}_2}(h)|. \quad (8)$$

Next, we formally introduce the statistical setting of our analytical investigation of the impact of group-aware hypothesis inference in a multi-client setting. For clients $i \in [M]$, let \mathcal{D}_i denote their corresponding distributions of data pairs (X, Y) . We assume that each local distribution \mathcal{D}_i is a mixture of group-specific

distributions $\mathcal{D}_g^i, g \in [G]$ for G . Concretely,

$$\mathcal{D}_i = \sum_{g \in [G]} \pi_g^i \mathcal{D}_g^i, \quad (9)$$

with mixing probability vector $[\pi_1^i, \dots, \pi_G^i]$. This also induces a probability distribution \mathcal{C}_g of data belonging to group g as follows:

$$\mathcal{C}_g = \sum_{i \in [M]} \pi_g^i \mathcal{D}_g^i. \quad (10)$$

Following [10], we refer to the distribution \mathcal{C}_g as the participated client's data distribution for the g -th group. In our setting, the group assignment formalized above corresponds to the execution of the function $\text{Select}: \mathcal{X} \rightarrow [G]$ assigning data to different groups.

We will also consider the empirical versions of the above distributions. Formally, let $\hat{\mathcal{D}}_i$ the induced local empirical distribution of client i by sampling N_g^i iid samples from each \mathcal{D}_g^i . Further, let $N_i = \sum_{g \in [G]} N_g^i$ denote the total number of samples per client and $N_g = \sum_{i=1}^M N_g^i$ denote the total number of data samples from group g . Onwards, we assume that the mixture weights in (9) are set as $\pi_g^i = N_g^i/N_i$. Thus, we also define the empirical distribution $\hat{\mathcal{C}}_g$ of each group as $\hat{\mathcal{C}}_g = \sum_{i \in [M]} \pi_g^i \hat{\mathcal{D}}_g^i = \sum_{i \in [M]} \frac{N_g^i}{N_i} \hat{\mathcal{D}}_g^i$. Finally, given a set $\{h_1, \dots, h_G\}$ of G hypotheses $h_g \in \mathcal{H}, g \in [G]$ one corresponding to each group, we denote h_{Select} the group-aware (data-point dependent) hypothesis determined by the Select function. In other words, $h_{\text{Select}} = \{h_1, \dots, h_G\}_{\text{Select}(x)}$ denotes a hypothesis that when acting on datapoint x returns $h_{\text{Select}(x)}$, for a fixed function $\text{Select}: \mathcal{X} \rightarrow [G]$.

C.2 Lemmas

In this section, we cover some technical lemmas which are useful for proving our main result. Lemma C.1 below splits the participated clients' distribution risk into the risks of each individual's group.

Lemma C.1 (Split the distribution risk). *Let fixed function $\text{Select}: \mathcal{X} \rightarrow \{1, \dots, G\}$. For the group-aware hypothesis h_{Select} that selects among hypotheses $\{h_1, \dots, h_G\}$, it holds for any client $i \in [M]$ that*

$$\mathcal{L}_{\mathcal{D}_i}(h_{\text{Select}}) = \sum_{g=1}^G \frac{N_g^i}{N_i} \mathcal{L}_{\mathcal{D}_g^i}(h_g).$$

Proof. By definition of the population risk:

$$\mathcal{L}_{\mathcal{D}_i}(h_{\text{Select}}) = \mathbb{E}_{(x,y) \sim \mathcal{D}_i}[\ell(h_{\text{Select}}, x, y)].$$

The desired follows from this by recalling the decomposition in (9) with weights mixing weights $\pi_g^i = \frac{N_g^i}{N_i}$. \square

The next lemma is useful to derive global and local performance gap.

Lemma C.2 (Bound on the generalization error). *Assume the loss is bounded in $[0, 1]$ and fix any client $i \in [M]$. Then with probability at least $1 - \delta$ over the training set,*

$$\begin{aligned} & \sum_{g=1}^G \frac{N_g^i}{N_i} \min_{h_g \in \mathcal{H}} \mathcal{L}_{\mathcal{C}_g}(h_g) - \sum_{g=1}^G \frac{N_g^i}{N_i} \min_{h_g \in \mathcal{H}} \mathcal{L}_{\hat{\mathcal{C}}_g}(h_g) \\ & \leq 2 \sqrt{\frac{\log \frac{1}{\delta}}{N_i}} + \sum_{g=1}^G \frac{N_g^i}{N_i} \mathfrak{R}_{\mathcal{C}_g, N_g^i}(\mathcal{H}). \end{aligned} \quad (11)$$

Proof. For any set of real numbers a_1, \dots, a_q and b_1, \dots, b_1 observe that $\min_i a_i \leq \max_i a_i$ and $\min_i b_i = -\max_i -b_i$, we get

$$\min_i a_i - \min_i b_i \leq \max_i (a_i - b_i).$$

Using this it holds that

$$\begin{aligned} & \sum_{g=1}^G \frac{N_g^i}{N_i} \min_{h_g \in H} \mathcal{L}_{\mathcal{C}_g}(h_g) - \sum_{g=1}^G \frac{N_g^i}{N_i} \min_{h_g \in H} \mathcal{L}_{\hat{\mathcal{C}}_g}(h_g) \\ & \leq \sum_{g=1}^G \frac{N_g^i}{N_i} \max_{h_g} \left(\mathcal{L}_{\mathcal{C}_g}(h_g) - \mathcal{L}_{\hat{\mathcal{C}}_g}(h_g) \right). \end{aligned}$$

Since the loss is bounded in $[0, 1]$, changing one sample changes the above term by at most one. Thus, by the McDiarmid's inequality, with probability at least $1 - \delta$,

$$\begin{aligned} & \sum_{g=1}^G \frac{N_g^i}{N_i} \max_{h_g} \left(\mathcal{L}_{\mathcal{C}_g}(h_g) - \mathcal{L}_{\hat{\mathcal{C}}_g}(h_g) \right) \\ & \leq \frac{1}{N_i} \mathbb{E} \left[\sum_{g=1}^G N_g^i \max_{h_g} \left(\mathcal{L}_{\mathcal{C}_g}(h_g) - \mathcal{L}_{\hat{\mathcal{C}}_g}(h_g) \right) \right] \quad (12) \\ & + \sqrt{\frac{1}{N_i} \log \frac{1}{\delta}}. \end{aligned}$$

Moreover, note that:

$$\begin{aligned} & \mathbb{E} \left[\sum_{g=1}^G \frac{N_g^i}{N_i} \max_{h_g} \left(\mathcal{L}_{\mathcal{C}_g}(h_g) - \mathcal{L}_{\hat{\mathcal{C}}_g}(h_g) \right) \right] \\ & = \sum_{g=1}^G \frac{N_g^i}{N_i} \mathbb{E} \left[\max_{h_g} \left(\mathcal{L}_{\mathcal{C}_g}(h_g) - \mathcal{L}_{\hat{\mathcal{C}}_g}(h_g) \right) \right] \\ & \leq 2 \sum_{g=1}^G \frac{N_g^i}{N_i} \mathfrak{R}_{\mathcal{C}_g, N_g}(\mathcal{H}). \quad (13) \end{aligned}$$

Combining Eq. (12) and Eq. (13), completes the proof. \square

C.3 Proof of Theorem 1

We are now ready to prove Theorem 5.1.

Proof. Given Lemma C.1, we split the distribution risk. Thus, the global-to-local performance gap becomes

$$\sum_{g=1}^G \frac{N_g^i}{N_i} \mathcal{L}_{\hat{\mathcal{D}}_g^i}(\hat{h}_g) - \min_{h \in H} \mathcal{L}_{\mathcal{D}_i}(h),$$

where $\hat{h}_g = \arg \min_{h \in H} \mathcal{L}_{\hat{\mathcal{C}}_g}(h)$ denote the empirical model for data group g . Next, observe from (9) that

$$\begin{aligned} \min_{h \in H} \mathcal{L}_{\mathcal{D}_i}(h) & = \min_{h \in H} \sum_{g=1}^G \frac{N_g^i}{N_i} \mathcal{L}_{\mathcal{D}_g^i}(h) \\ & \geq \sum_{g=1}^G \frac{N_g^i}{N_i} \min_{h_g \in H} \mathcal{L}_{\mathcal{D}_g^i}(h_g). \end{aligned}$$

Denote $\overline{h}_{g_i}^* = \min_{h_g \in H} \mathcal{L}_{\mathcal{D}_g^i}(h_g)$, we then get the following:

$$\begin{aligned} & \sum_{g=1}^G \frac{N_g^i}{N_i} \mathcal{L}_{\hat{\mathcal{D}}_g^i}(\hat{h}_g) - \min_{h \in H} \mathcal{L}_{\mathcal{D}_i}(h) \\ & \leq \sum_{g=1}^G \frac{N_g^i}{N_i} \mathcal{L}_{\hat{\mathcal{D}}_g^i}(\hat{h}_g) - \sum_{g=1}^G \frac{N_g^i}{N_i} \min_{h_g \in H} \mathcal{L}_{\mathcal{D}_g^i}(h_g) \\ & = \sum_{g=1}^G \frac{N_g^i}{N_i} \mathcal{L}_{\hat{\mathcal{D}}_g^i}(\hat{h}_g) - \sum_{g=1}^G \frac{N_g^i}{N_i} \left[\mathcal{L}_{\mathcal{C}_g}(h_{g_i}^*) + \mathcal{L}_{\mathcal{D}_g^i}(h_{g_i}^*) - \mathcal{L}_{\mathcal{C}_g}(h_{g_i}^*) \right] \\ & = \sum_{g=1}^G \frac{N_g^i}{N_i} \mathcal{L}_{\hat{\mathcal{D}}_g^i}(\hat{h}_g) - \sum_{g=1}^G \frac{N_g^i}{N_i} \left[\mathcal{L}_{\mathcal{C}_g}(h_{g_i}^*) + \mathcal{L}_{\mathcal{D}_g^i}(h_{g_i}^*) - \mathcal{L}_{\mathcal{C}_g}(h_{g_i}^*) \right] \\ & \quad - \sum_{g=1}^G \frac{N_g^i}{N_i} \mathcal{L}_{\hat{\mathcal{C}}_g}(\hat{h}_g) + \sum_{g=1}^G \frac{N_g^i}{N_i} \mathcal{L}_{\hat{\mathcal{C}}_g}(\hat{h}_g) \\ & = \sum_{g=1}^G \frac{N_g^i}{N_i} \mathcal{L}_{\hat{\mathcal{D}}_g^i}(\hat{h}_g) - \sum_{g=1}^G \frac{N_g^i}{N_i} \mathcal{L}_{\hat{\mathcal{C}}_g}(\hat{h}_g) \\ & \quad + \sum_{g=1}^G \frac{N_g^i}{N_i} \left(\mathcal{L}_{\mathcal{C}_g}(h_{g_i}^*) - \mathcal{L}_{\mathcal{D}_g^i}(h_{g_i}^*) \right) \\ & \quad + \sum_{g=1}^G \frac{N_g^i}{N_i} \mathcal{L}_{\hat{\mathcal{C}}_g}(\hat{h}_g) - \sum_{g=1}^G \frac{N_g^i}{N_i} \mathcal{L}_{\mathcal{C}_g}(h_{g_i}^*) \quad (14) \end{aligned}$$

Observing that $\sum_{g=1}^G \frac{N_g^i}{N_i} \min_{h_g \in H} \mathcal{L}_{\mathcal{C}_g}(h_g) \leq \sum_{g=1}^G \frac{N_g^i}{N_i} \mathcal{L}_{\mathcal{C}_g}(h_{g_i}^*)$ we get

$$\begin{aligned} (17) & \leq \sum_{g=1}^G \frac{N_g^i}{N_i} \max_{h_g \in H} \left| \mathcal{L}_{\mathcal{D}_g^i}(h_g) - \mathcal{L}_{\mathcal{C}_g}(h_g) \right| \\ & \quad + \sum_{g=1}^G \frac{N_g^i}{N_i} \max_{h_g \in H} \left| \mathcal{L}_{\hat{\mathcal{D}}_g^i}(h_g) - \mathcal{L}_{\hat{\mathcal{C}}_g}(h_g) \right| \\ & \quad + \sum_{g=1}^G \frac{N_g^i}{N_i} \min_{h_g \in H} \mathcal{L}_{\hat{\mathcal{C}}_g}(h_g) - \sum_{g=1}^G \frac{N_g^i}{N_i} \min_{h_g \in H} \mathcal{L}_{\mathcal{C}_g}(h_g). \end{aligned}$$

Then, combining lemma C.2, absolute homogeneity of Rademacher complexity, and the definition of the discrepancy in Eq. (8), we will have with probability $1 - \delta$,

$$\begin{aligned} & \sum_{g=1}^G \frac{N_g^i}{N_i} \mathcal{L}_{\hat{\mathcal{D}}_g^i}(\hat{h}_g) - \min_{h \in H} \mathcal{L}_{\mathcal{D}_i}(h) \quad (15) \\ & \leq \sqrt{\frac{\log \frac{1}{\delta}}{N_i}} + 2 \sum_{g=1}^G \frac{N_g^i}{N_i} \mathfrak{R}_{\mathcal{C}_g, N_g}(\mathcal{H}) \\ & \quad + \sum_{g=1}^G \frac{N_g^i}{N_i} \left(\text{disc}(\mathcal{D}_g^i, \mathcal{C}_g) + \text{disc}(\hat{\mathcal{D}}_g^i, \hat{\mathcal{C}}_g) \right) \quad (16) \end{aligned}$$

This completes the proof of Theorem 5.1. \square

C.4 Performance Gap on Real Distribution

In this section, we give the gap between the population loss of the global model found by empirical loss minimization using the Select grouping function and the population loss of the optimal model of client i : $\mathcal{L}_{\mathcal{D}_i}(\hat{h}_{\text{Select}}) - \min_{h \in H} \mathcal{L}_{\mathcal{D}_i}(h)$.

Proof. we follow the proof in [1]:

$$\begin{aligned}
\mathcal{L}_{\mathcal{D}^i}(\hat{h}_g) &\leq \sum_{g=1}^G \frac{N_g^i}{N_i} \mathcal{L}_{\mathcal{C}_g}(\hat{h}_g) + \mathcal{L}_{\mathcal{D}^i}(\hat{h}_g) - \sum_{g=1}^G \frac{N_g^i}{N_i} \mathcal{L}_{\mathcal{C}_g}(\hat{h}_g) \\
&= \sum_{g=1}^G \frac{N_g^i}{N_i} \mathcal{L}_{\mathcal{C}_g}(\hat{h}_g) + \sum_{g=1}^G \frac{N_g^i}{N_i} \mathcal{L}_{\mathcal{D}_g^i}(\hat{h}_g) \\
&\quad - \sum_{g=1}^G \frac{N_g^i}{N_i} \mathcal{L}_{\mathcal{C}_g}(\hat{h}_g) \\
&= \sum_{g=1}^G \frac{N_g^i}{N_i} \mathcal{L}_{\mathcal{C}_g}(\hat{h}_g) + \sum_{g=1}^G \frac{N_g^i}{N_i} \text{disc}(\mathcal{D}_g^i, \mathcal{C}_g) \\
&\leq \sum_{g=1}^G \frac{N_g^i}{N_i} \mathcal{L}_{\hat{\mathcal{C}}_g}(\hat{h}_g) + \sum_{g=1}^G \frac{N_g^i}{N_i} \text{disc}(\mathcal{D}_g^i, \mathcal{C}_g) \\
&\quad + \sum_{g=1}^G \frac{N_g^i}{N_i} \left(\mathcal{L}_{\mathcal{C}_g}(\hat{h}_g) - \mathcal{L}_{\hat{\mathcal{C}}_g}(\hat{h}_g) \right) \\
&\leq \sum_{g=1}^G \frac{N_g^i}{N_i} \mathcal{L}_{\hat{\mathcal{C}}_g}(\hat{h}_g) + \sum_{g=1}^G \frac{N_g^i}{N_i} \text{disc}(\mathcal{D}_g^i, \mathcal{C}_g) \\
&\quad + \sum_{g=1}^G \frac{N_g^i}{N_i} \max_{h_g} \left(\mathcal{L}_{\mathcal{C}_g}(h_g) - \mathcal{L}_{\hat{\mathcal{C}}_g}(h_g) \right) \\
&\leq \sum_{g=1}^G \frac{N_g^i}{N_i} \mathcal{L}_{\mathcal{C}_g}(h_{g_i}^*) + \sum_{g=1}^G \frac{N_g^i}{N_i} \text{disc}(\mathcal{D}_g^i, \mathcal{C}_g) \\
&\quad + \left| \sum_{g=1}^G \frac{N_g^i}{N_i} \left(\mathcal{L}_{\hat{\mathcal{C}}_g}(h_{g_i}^*) - \mathcal{L}_{\mathcal{C}_g}(h_{g_i}^*) \right) \right| \\
&\quad + \sum_{g=1}^G \frac{N_g^i}{N_i} \max_{h_g} \left(\mathcal{L}_{\mathcal{C}_g}(h_g) - \mathcal{L}_{\hat{\mathcal{C}}_g}(h_g) \right) \\
&\leq \sum_{g=1}^G \frac{N_g^i}{N_i} \mathcal{L}_{\mathcal{C}_g}(h_{g_i}^*) + \sum_{g=1}^G \frac{N_g^i}{N_i} \text{disc}(\mathcal{D}_g^i, \mathcal{C}_g) \\
&\quad + 2 \sum_{g=1}^G \frac{N_g^i}{N_i} \max_{h_g} \left(\mathcal{L}_{\mathcal{C}_g}(h_g) - \mathcal{L}_{\hat{\mathcal{C}}_g}(h_g) \right) \\
&\leq \sum_{g=1}^G \frac{N_g^i}{N_i} \mathcal{L}_{\mathcal{D}_g^i}(h_{g_i}^*) + \sum_{g=1}^G \frac{N_g^i}{N_i} \text{disc}(\mathcal{D}_g^i, \mathcal{C}_g) \\
&\quad + 2 \sum_{g=1}^G \frac{N_g^i}{N_i} \max_{h_g} \left(\mathcal{L}_{\mathcal{C}_g}(h_g) - \mathcal{L}_{\hat{\mathcal{C}}_g}(h_g) \right) \\
&\leq \sum_{g=1}^G \frac{N_g^i}{N_i} \mathcal{L}_{\mathcal{D}_g^i}(h_{g_i}^*) + 2 \sum_{g=1}^G \frac{N_g^i}{N_i} \text{disc}(\mathcal{D}_g^i, \mathcal{C}_g) \\
&\quad + 2 \sum_{g=1}^G \frac{N_g^i}{N_i} \max_{h_g} \left(\mathcal{L}_{\mathcal{C}_g}(h_g) - \mathcal{L}_{\hat{\mathcal{C}}_g}(h_g) \right) \tag{17}
\end{aligned}$$

Then, combining lemma C.2, absolute homogeneity of Rademacher complexity, and the definition of the discrepancy

in Eq. (8), we will have

$$\begin{aligned}
&\sum_{g=1}^G \frac{N_g^i}{N_i} \mathcal{L}_{\mathcal{D}_g^i}(\hat{h}_g) - \min_{h \in \mathcal{H}} \mathcal{L}_{\mathcal{D}_i}(h) \\
&\leq 2 \sqrt{\frac{\log \frac{1}{\delta}}{N_i}} + 4 \sum_{g=1}^G \frac{N_g^i}{N_i} \mathfrak{R}_{\mathcal{C}_g, N_g}(\mathcal{H}) \\
&\quad + 2 \sum_{g=1}^G \frac{N_g^i}{N_i} \text{disc}(\mathcal{D}_g^i, \mathcal{C}_g)
\end{aligned} \tag{18}$$

□

Thus we got the following theorem:

Theorem C.3. Assume the loss function ℓ is bounded in $[0, 1]$ and the function *Select* is a data grouping method. Let $\mathfrak{R}_{\mathcal{D}, m}(\mathcal{H})$ represent the Rademacher complexity of the hypothesis class \mathcal{H} over the distribution \mathcal{D} with m samples. Then, with a probability of at least $1 - \delta$ over the training set,

$$\begin{aligned}
&\mathcal{L}_{\mathcal{D}_i}(\hat{h}_{\text{Select}}) - \min_{h \in \mathcal{H}} \mathcal{L}_{\mathcal{D}_i}(h) \\
&\leq 2 \sqrt{\frac{\log \frac{1}{\delta}}{N_i}} + 4 \sum_{i=1}^G \frac{N_g^i}{N_i} \mathfrak{R}_{\mathcal{C}_g, N_g}(\mathcal{H}) \\
&\quad + \sum_{g=1}^G \frac{N_g^i}{N_i} \left(2 \text{disc}(\mathcal{D}_g^i, \mathcal{C}_g) \right),
\end{aligned} \tag{19}$$

where $\text{disc}_{\mathcal{H}}(\mathcal{D}_1, \mathcal{D}_2) = \max_{h \in \mathcal{H}} |\mathcal{L}_{\mathcal{D}_1}(h) - \mathcal{L}_{\mathcal{D}_2}(h)|$.

The obtained theorem also suggests that tuning G is important in achieving optimal performance, which agrees with theorem 5.1.

D Additional Experiments

In this section, we will first discussed additional comparison results (Section D.1), which include an extra heterogeneity setting and learning curves of different methods. We will then introduce an additional ablation study (Section D.2) and evaluate the efficiency of FGPT (Section D.3). Finally, we will analyze the prompts in Section D.4.

D.1 More Comparison with Baselines

Dirichlet Partition

In this section, we report results with "Dirichlet Partition" on CIFAR-100 dataset. We follow the approach outlined in [27], which employs a two-stage Pachinko allocation method to partition samples over "coarse" and "fine" labels. This method first generates a Dirichlet distribution with parameter β over the coarse labels for each client and then generates a Dirichlet distribution with parameter $\beta_f = 10$ over the coarse corresponding fine labels. We report results with heterogeneity $\beta \in \{0.1, 0.01\}$ in Table 7. FGPT and FGPT-U consistently perform better. Moreover, our method is robust to heterogeneity, which does not significantly affect the performance even when β is reduced (heterogeneity is increased).

Learning Curves

The accuracy curve, defined as the accuracy across different communication rounds, is an important factor in demonstrating the convergence of the algorithm. Figure 3 shows test accuracy curves

Table 7: Performance comparison of different methods on the CIFAR-100 Dataset with Dirichlet partition. We report the averaged testing accuracy for the last 10 consecutive global communication rounds and compute the mean test accuracy and variance over these evaluation steps to estimate the model performance.

FL settings			Accuracy						
β	γ	E	Ours	Ours-U	PT-FedAvg	pFedHN	Fed-DualPrompt	FedMoon	FedMix
0.1	0.05	5	82.91 (0.11)	83.88 (0.01)	82.57 (0.26)	80.84 (1.07)	81.74 (0.52)	82.87 (0.14)	80.08 (1.35)
0.01	0.05	5	80.92 (0.54)	82.01 (0.25)	77.75 (0.99)	76.46 (2.21)	80.09 (1.01)	78.97 (0.03)	79.70 (0.04)

Table 8: Performance comparison of different methods on the CIFAR-100 with $E = 2$ and $E = 5$. We report the averaged testing accuracy for the last 10 consecutive global communication rounds and compute the mean test accuracy and variance over these evaluation steps to estimate the model performance.

FL settings			Accuracy \uparrow						
Dataset	s	E	FGPT	FGPT-U	PT-FedAvg	pFedHN	Fed-DualPrompt	FedMoon	FedMix
CIFAR-100	10	2	78.81 (0.07)	79.92 (0.04)	77.29 (0.33)	76.03 (0.27)	77.48 (0.41)	77.54 (0.32)	78.51 (0.16)
	10	5	81.09 (0.40)	82.45 (0.39)	78.29 (1.46)	76.86 (0.95)	78.91 (0.93)	79.39 (0.53)	80.23 (0.40)
	5	2	76.76 (0.53)	77.58 (0.48)	71.99 (2.64)	71.06 (2.04)	71.04 (0.92)	70.89 (2.69)	73.10 (2.08)
	5	5	78.32 (0.35)	80.15 (0.14)	72.44 (3.52)	72.62 (2.73)	73.51 (2.97)	74.80 (3.17)	75.51 (1.81)

Table 9: Performance when combine FGPT with FedMix.

FL settings		Accuracy		
dataset	s	Ours	FedMix	Ours + FedMix
CIFAR-100	10	81.09 (0.40)	80.52 (0.41)	81.64 (0.57)
CIFAR-100-C	10	70.89 (0.26)	71.01 (0.17)	71.40 (0.30)

using $\gamma = 0.05$, $E = 5$ for different heterogeneity levels. Specifically, we present the results for $s = 5$ and $s = 10$ with dashed and solid lines, respectively. It is evident that FGPT exhibits faster convergence compared to other methods. At last, FGPT are more robust to extremely heterogeneous data, with $s = 5$ surpassing baseline methods by a significant margin.

Combination with Other FL methods

It is also notable that our proposed FGPT can be combined with other strong heterogeneous FL methods that are orthogonal to FGPT, *e.g.*, FedMix [37]. Note that FedMix is the best baseline method in comparison (see Table 1) that provides an approximation of global Mixup by using exchanged and averaged local data to handle data heterogeneity issues. Here, we show that integrating the data sharing strategy in FedMix with FGPT’s training and inference strategies to further improve performance (see Table. 9).

D.2 More Ablation Study

Local Epoch E

In this section, we examine the different choices of *Local Epochs* (E) on the CIFAR-100 dataset. We use the same number of communication rounds (60) for experiments with $E = 2$ and $E = 5$. As shown in Table 8, our methods consistently outperform the baseline lines on averaged accuracy. Furthermore, we observed that a smaller value of E achieves reduced accuracy variance, indicating a smaller dissimilarity in model weights and stable training progress, however, leading to lower accuracy compared with large E as the total local training iteration is smaller. In addition, our method achieved the smallest accuracy variance, suggesting that it is more stable during training compared to the other methods.

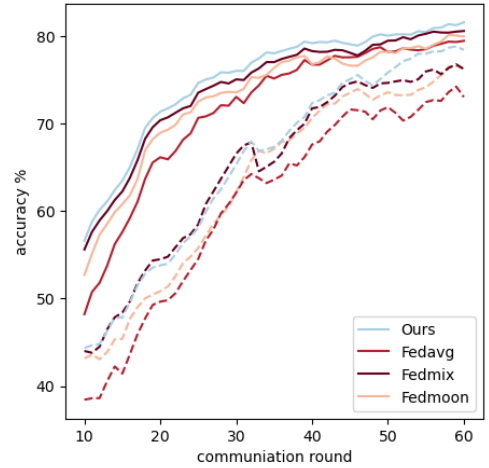


Figure 3: CIFAR-100 accuracy curve with local epoch $E = 5$. The dashed line and solid line are results for $s = 5$ and $s = 10$ respectively.

D.3 The Efficiency of FGPT

In this section, we analyze the efficiency of FGPT and introduce a lightweight variant of FGPT, called FGPT-ResNet. *Firstly*, to help understand the level of the computational cost of FGPT, we include the costs for alternative benchmarks in Table 10, which outlines the FLOPs of different steps for one testing and training sample. It is noteworthy that these benchmark non-iid FL techniques are computational-heavy during the training stage over *multiple training iterations* T . To be specific, FedMix [37] involves computing gradients with respect to input images, thereby doubling the training costs. pFedHN [29] necessitates training an added hyper-network, and FedMoon [17] involves embedding contrastive learning, which introduces extra gradient computations. In contrast, the additional cost of FGPT during training arises solely from generating embeddings for prompt selection *once* inference (refer to step 1 in Algorithm 2). As shown in Table 10, the total FLOPs for T -update training and one inference of FGPT could remain relatively low when the total training updates T is large. *Secondly*, in contrast to the other PFL methods involving additional fine-tuning on local clients —resulting in increased training costs— our FGPT is a finetuning-free strategy.

Table 10: Resources cost, our costs remain relatively low during training time and slightly increased during inference time. The total FLOPs for T -update training and one inference of FGPF could remain relatively low when the total training updates T is large. For efficiency, a lighter-weighted embedding encoder could be considered (*i.e.*, Ours-ResNet). The Performance if Ours-ResNet is competitive to baselines.

Method	Testing FLOPs (M)	Training FLOPs (M) / update	Embedding Inference FLOPs (M)	Total FLOPs (M) with T updates and 1 inference	Accuracy CIFAR-100, $s = 10$
Ours	33.11	39.24	16.55	$33.11 + 16.55 + 39.24 * T$	81.09 (0.40)
Ours-ResNet	22.44	39.24	4.13	$22.44 + 4.12 + 39.24 * T$	80.53 (0.64)
FedMix	18.31	74.39	N/A	$18.31 + 74.39 * T$	80.23 (0.40)
FedMoon	18.31	43.66	N/A	$18.31 + 43.66 * T$	79.39 (0.53)
pFedHN	18.31	60.12	N/A	$18.31 + 60.12 * T$	76.86 (0.95)

Table 11: Investigating performance on prompt similarity across clients. A larger shared prompt similarity means smaller gradient dissimilarity among clients. Local group similarity measures each group prompt’s similarity. The global group similarity represents the specificity of the prompt.

Method $\gamma = 0.05, E = 2, s = 10$	Prompt Similarity			Performance
	shared \uparrow	group (global) \downarrow	group (local) \uparrow	Accuracy \uparrow
PT-Fedavg-share	0.8334	–	–	77.51(0.24)
PT-Fedavg	0.8128	–	0.9491	77.29(0.33)
Fed-DualPrompt	0.8329	0.0377	0.9755	77.48(0.11)
Ours	0.8462	0.0349	0.9758	78.81(0.07)

For instance, when dealing with novel clients, [21] mandates employing all models to conduct inference across the complete local data and then selecting the optimal model. Similarly, in the scenario presented by [22], the workload of participating clients increases in correlation with the number of clusters. *Thirdly*, we want to highlight that our *extra costs* remain at a constant order $O(1)$ (one extra embedding inference pass) compared to FedAvg, and this cost can be reduced by using a lighter-weighted feature extractor to generate embeddings in the prompt selection module. We implemented a ResNet50 for prompt selection, and the FLOPs cost and performance are reported in Table 10. Despite the utilization of a lighter extractor, the performance remains consistently strong.

D.4 Prompt Analysis

Our study in this section primarily investigated the diversity of prompts utilized by various clients in FL. To evaluate similarity, we used three metrics: (1) shared similarity is denoted by mean similarity across all clients’ shared prompts after local updates. (2) global group similarity is denoted by the similarity within group prompts that obtained from the global model. (3) local group similarity is calculated by averaging the similarity between each client’s corresponding local updated group prompt.

Benefit of Group-Aware Prompts.

The group-aware prompt methods are introduced to alleviate the distribution dissimilarity problem. As shown in Table 11, if we add prompts to the same position as both shared and group prompts in FGPF and train with FedAvg (denoted as PT-FedAvg), the shared prompt similarity drops by 2.1% compared with FedAvg with shared prompts only (denoted as PT-FedAvg-shared). The reason behind this is group prompts’ layer is a higher layer which is more specialized and the effect of the heterogeneity is stronger [38], thus improvement should be implemented to resolve the problem. With the help of group-aware prompts, Fed-DualPrompt [35] improves the shared dissimilarity and local group similarity by about 2.0% and 2.6% respectively compared with the PT-Fedavg. However, it still has lower shared similarity compared to PT-Fedavg-

share. This is because data distribution in FL shifts throughout the learning process, which makes the learning of the clustering function in Fed-DualPrompt unstable and harms performance. It is notable that our method FGPF that clusters data with fixed orthogonal keys successfully achieves the best shared and local group similarity scores and, in addition, obtains a smaller global group similarity which indicates group prompts are more specialized.